Practical approaches for crystal structure predictions with inpainting generation and universal interatomic potentials

Peichen Zhong[a], **Xinzhe Dai**[a], **Bowen Deng**[a], **Gerbrand Ceder**[a], **Kristin A. Persson**[a]

[a] *University of California Berkeley, California 94720, United States* zhongpc@berkeley.edu

* Presenting author

1. Introduction

Recent advances in graph neural network (GNN) models offer promising alternatives to crystal structure prediction (CSP) problems. Universal machine learning interatomic potentials (uMLIPs) trained on millions of DFT calculations demonstrate remarkable generalizability in materials discovery. On the other hand, deep generative models (e.g., diffusion models) learn the data manifold or probabilistic distribution and generate new configurations via stochastic or variational approaches [1, 2], e.g., Xie et al. [3] introduced CDVAE as the first GNN-based diffusion model for crystal structure generations.

We found that GNN-based models suffer from locality bias when generating structures at large scales. Although GNN can successfully learn short and medium-range atomic correlations, the generated structures often exhibit amorphous configurations rather than proper crystalline order. This bias stems from GNNs' finite receptive field limitation and the stochastic nature of reverse diffusion processes, which sample from broad distributions resulting in "mosaics" of disconnected local structure motifs.

2. Substantial section

We present Crystal Host-Guided Generation (CHGGen) as a practical approach for crystal structure prediction based on diffusion models. Our research reveals that unconditional generation with GNN-based diffusion models demonstrates limited efficacy in identifying symmetrized crystals as unit cell size increases. CHGGen addresses this limitation through conditional generation using the inpainting method, which optimizes a fraction of atomic positions within a predefined and symmetrized host structure. We used CHGNet as a uMLIP for structure optimization and virtual screening of thermodynamic stability of generated structures, which are subsequently validated using density functional theory calculations.

2.1 Related work

- **Universal machine learning interatomic potentials**: M3GNet [4], CHGNet [5], MACE [6], GNoME [7], MatterSim [8], DPA-2 [9].
- **GNN-based diffusion models**: CDVAE [3], DiffCSP [10], MatterGen [11], symmetry-constrained diffusion [12].
- **Materials database**: Materials Project [13] and Alexandria [14], OMAT24 [15].
- **Generative models for materials beyond GNN**: U-net-based diffusion models [16], large-language models [17, 18], and Wyckoff-based generators [19, 20, 21].

2.2 Inpainting generation

Inpainting Generation. Inputs: Atomic positions of unperturbed host structure with randomly initialized intercalants $\boldsymbol{x}_0^{\text{host}}$; Atomic positions of all atoms sampled randomly in the unit cell $\boldsymbol{x}_T$; Mask for intercalants m; Signal-to-noise ratio δ; Number of predictor steps T; Number of corrector steps M; Number of resampling steps r.

for $t = T, \cdots, 1$ **do**
  for $n = 1, \cdots, r$ **do**
    $\boldsymbol{x}_{t-1} \leftarrow \boldsymbol{x}_t + (\sigma_t^2 - \sigma_{t-1}^2)\boldsymbol{s}_\theta(\boldsymbol{x}_t, t)$
    $\boldsymbol{z} \sim \mathcal{N}(\mathbf{0}, \mathbf{I})$
    $\boldsymbol{x}_{t-1} \leftarrow \boldsymbol{x}_{t-1} + \sqrt{\frac{\sigma_{t-1}^2(\sigma_t^2 - \sigma_{t-1}^2)}{\sigma_t^2}}\,\boldsymbol{z}$
    for $j = 1, \cdots, M$ **do**
      $\boldsymbol{z} \sim \mathcal{N}(\mathbf{0}, \mathbf{1})$
      $\boldsymbol{g} \leftarrow \boldsymbol{s}_\theta(\boldsymbol{x}_{t-1}, t-1)$
      $\epsilon \leftarrow 2(\sqrt{3}\delta / \|\boldsymbol{g}\|_2)^2$
      $\boldsymbol{x}_{t-1} \leftarrow \boldsymbol{x}_{t-1} + \epsilon\,\boldsymbol{g} + \sqrt{2\epsilon}\,\boldsymbol{z}$
    end for
    $\boldsymbol{x}_{t-1}^{\text{host}} \leftarrow \boldsymbol{x}_0^{\text{host}} + \sigma_{t-1}\boldsymbol{z}$
    $\boldsymbol{x}_{t-1} \leftarrow (1 - m) \odot \boldsymbol{x}_{t-1}^{\text{host}} + m \odot \boldsymbol{x}_{t-1}$
    if $n < r$ **and** $t > 1$ **then**
      $\boldsymbol{z} \sim \mathcal{N}(\mathbf{0}, \mathbf{1})$
      $\boldsymbol{x}_t \leftarrow \boldsymbol{x}_{t-1} + \sqrt{\sigma_{t-1}^2 - \sigma_{t-2}^2}\,\boldsymbol{z}$
    end if
  end for
end for

2.3 Crystal host-guided generation

The CHGGen computational workflow begins with sampling different Bravais lattices at a fixed volume by conducting a random search across lattice constants and angles. The unconditional diffusion proceeds by solving the reverse stochastic differential equations to generate structures. These structures undergo relaxation using CHGNet to optimize both unit cells and atomic coordinates.

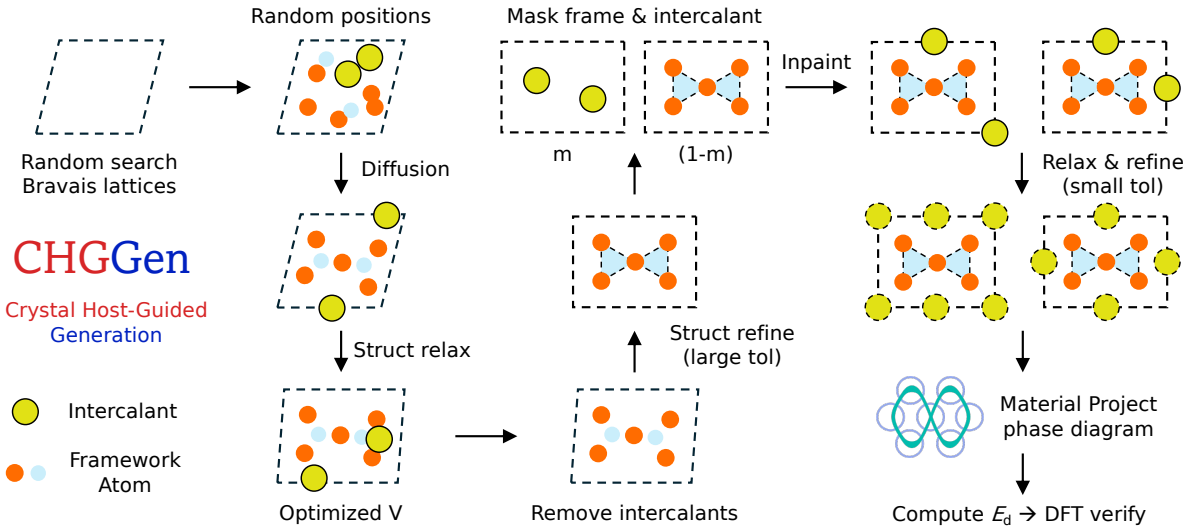

Fig. 1: **The computational workflow of CHGGen.** The process begins with a random search for Bravais lattices containing a specified number of atoms, followed by an unconditional generation with reverse diffusion and structure relaxation. Structure refinement is applied after removing intercalants to obtain a symmetrized framework. Inpainting generation is then performed based on this refined framework to guide the creation of complete crystal structures. Finally, the generated structures undergo relaxation to determine decomposition energy (E_d). The structures with low E_d are selected for DFT verification. The dashed circles represent crystallographically equivalent atomic positions in a crystal structure.

The next phase begins by removing atoms that exhibit broad local environment distributions. The remaining structure (framework) undergoes symmetry refinement using `spglib` through incremental structural matching tolerance to obtain a space group with higher symmetry. After that, fractional coordinates of the removed intercalants are then reinitialized from $\mathcal{N}(\mathbf{0}, \mathbf{I})$ within the symmetrized framework, and inpainting generation is performed using masks m and $(1 - m)$ for the intercalants and framework respectively. The inpainting-generated structures are further relaxed using CHGNet and structure refinement is performed with a small tolerance to obtain the spacegroup. The CHGNet-calculated energy is used to determine the decomposition energy E_d relative to the MP phase diagram. Finally, structures with E_d within a specified threshold are submitted to DFT calculations to get more accurate thermodynamic stability.

Acknowledgments

This work was supported by the U.S. Department of Energy under Contract No. DE-AC0205CH11231 (Materials Project program KC23MP) and National Energy Research Scientific Computing Center (NERSC) under the GenAI Project. P.Z. acknowledges funding support from the BIDMaP Postdoctoral Fellowship.

[1] Zekun Ren et al. In: *Matter* 5 (1 Jan. 2022), pp. 314–335. ISSN: 25902385.

[2] Hyunsoo Park, Anthony Onwuli, and Aron Walsh. In: *chemRxiv* (2024).

[3] Tian Xie et al. In: *International Conference on Learning Representations (ICLR)* (2021).

[4] Chi Chen and Shyue Ping Ong. In: *Nature Computational Science* 2.11 (Nov. 2022), pp. 718–728. ISSN: 2662-8457.

[5] Bowen Deng et al. In: *Nature Machine Intelligence* 5 (Sept. 2023), pp. 1031–1041. ISSN: 2522-5839.

[6] Ilyes Batatia et al. In: *arXiv:2401.00096* (2023).

[7] Amil Merchant et al. In: *Nature* 624.7990 (2023), pp. 80–85.

[8] Han Yang et al. In: *arXiv:2405.04967* (2024).

[9] Duo Zhang et al. In: *npj Comput. Mater.* 10.1 (2024), p. 293.

[10] Rui Jiao et al. In: *Advances in Neural Information Processing Systems (NeurIPS)* (2023).

[11] Claudio Zeni et al. In: *Nature* (Jan. 2025), pp. 1–56. ISSN: 0028-0836.

[12] Daniel Levy et al. In: *International Conference on Learning Representations (ICLR)* (2025).

[13] Anubhav Jain et al. In: *APL Materials* 1.1 (July 2013), p. 011002. ISSN: 2166-532X.

[14] Jonathan Schmidt et al. In: *Advanced Materials* 35.22 (June 2023). ISSN: 0935-9648.

[15] Luis Barroso-Luque et al. In: *arXiv:2410.12771* (2024).

[16] Sherry Yang et al. In: *arXiv:2311.09235* (2023).

[17] Nate Gruver et al. In: *International Conference on Learning Representations (ICLR)* (2024).

[18] Luis M. Antunes, Keith T. Butler, and Ricardo Grau-Crespo. In: *Nature Communications* 15.1 (Dec. 2024), p. 10570. ISSN: 2041-1723.

[19] Ruiming Zhu et al. In: *arXiv:2311.17916* (2023).

[20] Zhendong Cao et al. In: *arXiv:2403.15734* (2024).

[21] Nikita Kazeev et al. In: *arXiv:2503.02407* (2025).